Dalton Transactions

Accepted Manuscript

This article can be cited before page numbers have been issued, to do this please use: Y. Zhang, A. J. Brown, Y. Meng, H. Sun and S. Gao, *Dalton Trans.*, 2014, DOI: 10.1039/C4DT03545C.

ROYAL SOCIETY OF CHEMISTRY

www.rsc.org/dalton

Dynamic Article Links ▶
View Article Online
DOI: 10.1039/C4DT03545C

Cite this: DOI: 10.1039/c0xx00000x

www.rsc.org/xxxxxx

ARTICLE TYPE

Linear trinuclear cobalt(II) single molecule magnet

Yuan-Zhu Zhang,*[a] Andrew J Brown,[b] Yin-Shan Meng,[a] Hao-Ling Sun,[c] Song Gao*[a]

Received (in XXX, XXX) Xth XXXXXXXXX 20XX, Accepted Xth XXXXXXXXX 20XX
DOI: 10.1039/b000000x

Introduction of $NaBPh_4$ into a methanolic solution of $CoCl_2·6H_2O$ and 2-[(pyridine-2-ylimine)-methyl]phenol (Hpymp) afforded $\{[Co^{II}_3(pymp)_4(MeOH)_2][BPh_4]_2\}·2MeOH$ (**1**) with a centro-symmetrically linear trinuclear structure. Magnetic analysis of **1** exhibited significant intracluster ferromagnetic exchange (2.4 cm^{-1}) and slow relaxation of magnetization at both zero and non-zero static fields below 5 K, giving the first $[Co^{II}_3]$ single molecule magnet with an effective energy barrier of 17.2(3) cm^{-1} under 500 Oe dc field.

Introduction

In an Ising-like system, or when spin is a good quantum number, the combination of a large spin ground state (*S*) and uniaxial magnetic anisotropy (D < 0) can result in a single molecule magnet (SMM) with an energy barrier (U) to spin reversal: U = $|D|S^2$ or $|D|(S^2-1/4)$ for integer and half-integer spin, respectively. Extensive studies, both in theory and experiment, are on-going efforts with the aim for higher energy barriers that would allow practical applications in information storage.[1,2] In well-studied Mn(III)-SMMs, where the orbital contribution to magnetic moment in the Mn(III) ion is quenched, a common magneto-structural correlation has been documented. Namely, the parallel alignment of Jahn-Teller (*JT*) axes and ferromagnetic intracluster interactions lead to large anisotropy.[3] One drawback from such systems is the low magnitude of the axial zero-field splitting parameter for the Mn(III) ion, $D_{Mn} \approx -4$ cm^{-1}.[4] Thus, other metal ions with unquenched orbital angular momentum emanating from strong spin-orbital couplings have attracted more concerns.[5,6] The Co(II) ion has been of particular interest as a new anisotropy source in recent years.[7] The very recent progress on several series of mononuclear Co(II)-SMMs demonstrated large and tunable anisotropy with D_{Co} varying from -115 to +13 cm^{-1} afforded by deliberate modification on coordination geometry, degree of structural distortion, and ligand field strength.[8] Further incorporation of these high anisotropy ions into clusters with the potential for strong communication and favorable arrangement of the anisotropy vectors may stand for a new challenge in this field.[9] In this regard, structurally simple molecules (low-nuclearity) are currently of particular interest.

Among the known Co(II)-SMMs, the first and most well-studied are primarily those containing the cubane $[Co_4O_4]$ motif, in which orthogonal hard-axis alignments of four single-ion spins ($D_{Co} > 0$) were proposed to result in negative global D_{mol} values.[10] This concept was again manifest in a $[Co^{II}_7]$ SMM with two fused cubanes.[11] Another popular system is the planar $[Co_7]$ disc family of SMMs with a central cobalt ion surrounded by a ring of six cobalt ions.[12,13] However, this disc-like geometry suffers from the non-colinear alignment of magnetic anisotropies between the surrounding cobalt(II) ions, as evidenced by the mixed $[Co^{II}_4Co^{III}_3]$ disc[13a] exhibiting improved SMM properties over the $[Co^{II}_6Co^{III}]$ disc, which contained only one Co^{III} ion in the center.[13b]

In attempts to exploit a co-linear alignment of the anisotropy axes, we were inspired by a series of heterometallic linear $[Co^{II}_2Ln^{III}]$[14] and one linear $[Co^{II}_4]$[15] clusters that have been characterized as SMMs. In this regard, we targeted linear $[Co^{II}_3]$ SMMs, which hitherto remain unexplored.[16] Treatment of $CoCl_2·6H_2O$ and 2-[(pyridine-2-ylimine)methyl]phenol (Hpymp, Scheme 1) with $NaBPh_4$ in a methanolic solution afforded brown thin-plate crystals of $\{[Co^{II}_3(pymp)_4(MeOH)_2][BPh_4]_2\}·2MeOH$ (**1**), which consists of a centro-symmetric cationic array of three cobalt atoms ligated by four $[pymp]^-$ ligands. For comparison, $[Co^{II}_3(pymp)_4(pya)_2][ClO_4]_2$ (**2**, pya = pridine-2-amine) was also synthesized.[17] Magnetic analysis revealed that **1** exhibits significant intracluster ferromagnetic exchange (J = +2.4 cm^{-1}) and slow relaxation of magnetization at both zero and non-zero static fields below 5 K with an effective energy barrier of 17.2(3) cm^{-1} under 500 Oe dc field.

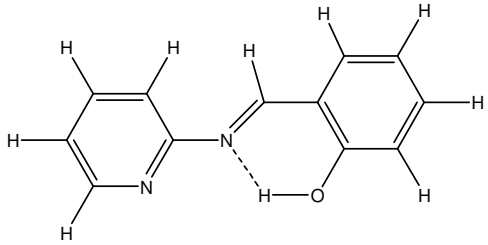

Scheme 1 2-[(pyridine-2-ylimine)methyl]phenol (Hpymp)

Experimental Section

Materials and Physical Measurements.

All starting materials were commercially available, reagent grade, and used as purchased without further purification. Elemental

View Article Online
DOI: 10.1039/C4DT03545C

analysis of carbon, hydrogen, and nitrogen were carried out with an Elementary Vario EL. The IR spectra were recorded on a Magna-IR 750 spectrophotometer in the 4000-500 cm^{-1} region. The measurements of magnetic properties were performed on an Oxford Maglab^{2000} System and a Quantum Design MPMS XL-7 SQUID magnetometer. The experimental susceptibilities were adjusted to correct for diamagnetic contributions (Pascal's tables).[18] All SQUID samples were immobilized in NMR tubes with eicosane for reducing possible magnetic torqueing.

Synthesis of Hpymp

Treatment of salicylalhehyde (2.44 g, 2.00 mol) and pya (1.88 g, 2.00 mol) in methanol (20 mL) afforded a yellow solution, which was stirred for 3 d. Yellow crystalline powder of Hpymp was obtained after removing the methanol by rotary evaporation, and drying under vacuum for 3 h. Yield: 3.60 g (90.9 %). Anal. Calcd $C_{12}H_{10}N_2O$ (M.W. = 198.22 g mol^{-1}): C, 72.71; H, 5.08; N, 14.13. Found: C, 72.58; H, 5.13; N, 14.09. IR (Nujol, cm^{-1}): 1614 (S) for ν(C=N) stretching vibration of Schiff base. The purity was also checked by NMR spectra ($CDCl_3$). (Fig. S1)

Synthesis of $\{[Co^{II}_3(pymp)_4(MeOH)_2][BPh_4]_2\}\cdot 2MeOH$ (1)

A 5 mL methanolic solution of Hpymp (95.5 mg, 0.482 mmol) was added to a 8 mL methanolic solution of $CoCl_2\cdot 6H_2O$ (72.5 mg, 0.305 mmol) to afford an orange solution, which was stirred for 2 min. $NaBPh_4$ (99.7 mg, 0.291 mmol) in methanol (3 ml) was added and the resulting solution was kept undisturbed overnight in air. Brown thin plate-like crystals of **1** were isolated via filtration, washed with methanol (5 mL), and dried in air. Yield: 115 mg (65.3 %). Anal. Calcd $C_{100}H_{92}B_2Co_3N_8O_8$: C, 69.34; H, 5.35; N, 6.47. Found: C, 69.87; H, 5.23; N, 6.58. IR (Nujol, cm^{-1}): ν_s(C=N) 1623 (s). Powder X-ray diffraction (PXRD) of **1** matched the simulated pattern from single crystal data. (Fig. S2)

Synthesis of $\{[Co^{II}_3(pymp)_4(pya)_2][ClO_4]_2\}$ (2)

Compound **2** was synthesized with a slightly modified procedure of the reported literature.[17] A 5 mL methanolic solution of Hpymp (85.5 mg, 0.431 mmol) and pya (26.5 mg, 0.282 mmol) was added to a 5 mL methanolic solution of $Co(ClO_4)_2\cdot 6H_2O$ (105.6 mg, 0.288 mmol). The resulting red solution was filtered and allowed to sit undisturbed overnight. Red block-like crystals were isolated via filtration, washed with methanol (5 mL), and dried in air. Yield: 75.5 mg (58.0 %). Anal. Calcd $C_{58}H_{48}Co_3Cl_2N_{12}O_{12}$: C, 51.50; H, 3.58; N, 12.42. Found: C, 51.65; H, 3.76; N, 12.49. The compound was confirmed by single crystal X-ray diffraction.

Caution! Perchlorate salts of metal complexes with organic compounds are potentially explosive. Only a small amount of material should be prepared and handled with great care.

Single Crystal structural data:

The diffraction data for **1** (0.25 × 0.14 × 0.04 mm) was collected at 293(2) K on a Nonius κ-CCD diffractometer (λ = 0.71073 Å). Initial cell parameters were obtained (DENZO) from ten 1° frames (SCALEPACK). Lorentz/polarization corrections were applied during data reduction and the structures were solved by the direct method (SHELXS-97). Refinements were performed by full-matrix least squares (SHELXL-97) on F^2 and empirical absorption corrections (SADABS) were applied. Anisotropic thermal parameters were used for the non-hydrogen atoms. Hydrogen atoms were added geometrically and refined using a riding model. Weighted R factors (*w*R) and all the goodness-of-fit (S) values are based on F^2; conventional R factors (R) are based on F, with F set to zero for negative F^2.

Table 1. Selected crystallographic data for **1** at 293(2) K.

formula	$C_{100}H_{92}B_2Co_3N_8O_8$
formula wt	1732.23
crystal system	Triclinic
space group	$P\bar{1}$
a, Å	11.5855(5)
b, Å	14.4488(6)
c, Å	15.1235(8)
α, deg	72.292(2)
β, deg	67.952(2)
γ, deg	69.590(2)
V, $Å^3$	2154.99(17)
D_c, g cm^{-3}	1.335
Z	1
μ, mm^{-1}	0.634
GOOF	0.834
R_1 ($I \geq 2\sigma(I)$)	0.0484
wR_2 ($I \geq 2\sigma(I)$)	0.0872

Table 2. Selected bond distances (Å) and angles (°) for **1**

Co1-O1	2.022(3)	O1-Co1-N1A	91.71(11)
Co1-O2	2.145(3)	O3-Co2-N3	92.86(13)
Co1-N1	2.124(3)	O3-Co2-N2	90.75(13)
Co2-N2	2.089(3)	O3-Co2-N4	86.89(13)
Co2-N3	2.018(3)	O3-Co2-O2	95.76(12)
Co2-N4	2.397(4)	O3-Co2-O1A	170.67(11)
Co2-O3	2.137(3)	N3-Co2-N4	59.88(14)
Co2-O2	2.038(3)	N2-Co2-O2	109.41(13)
Co2-O1A	2.118(3)	Co1-O1A-Co2	94.30(0)
O1-Co1-O1A	180.0 (1)	Co1-O2-Co2	93.02(0)
O1-Co1-O2	97.91(10)	Co1…Co2	3.036(1)
O1-Co1-O2A	82.09(10)	Co2…Co2A	6.072(3)
O1-Co1-N1	88.29(11)		
Symmetry transformations used to generate equivalent atoms: A -x,-y,-z+1;			

Results and discussion

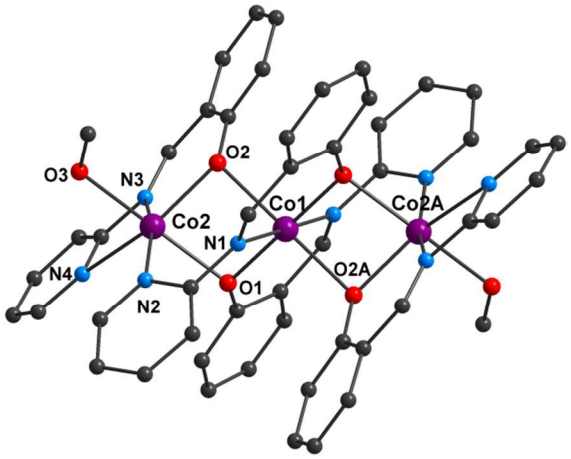

Fig. 1 Ball-and-stick view of X-ray structure of **1**. Counter anions of $[BPh_4]^-$, hydrogen atoms and lattice solvents are eliminated for clarity.

View Article Online
DOI: 10.1039/C4DT03545C

Description of structures

Compounds **1** and **2** crystallize in the triclinic $P\bar{1}$ space group and exhibit similar structures (Figs. 1 and S3). Compound **1** consists of a centro-symmetric cationic array of three cobalt atoms ligated by four [pymp]$^-$ ligands with dihedral angles between their phenyl and pyridine rings being 114.8° and 16.1° for the twisted (pymp_O1) and flattened (pymp_O2) ligands, respectively. The central Co1, which resides on an inversion center, displays a compressed octahedral geometry formed by two imino N atoms and four phenolate O atoms. The bond distance of the apical Co1-O1/O1A [2.022(3) Å] is significantly shorter than the equatorial distances [Co1-N/O = 2.124(3) – 2.145(3) Å]. The bond angles of *cis* O–Co1–O/N are in the range of 82.09(10) to 97.91(10)°. The outer cobalt atoms [Co2 and Co2A] adopt a highly distorted octahedral geometry with a [N_3O_3] environment due to coordination of one methanol molecule, one flat pymp ligand, and two twisted pymp ligands. The flat pymp ligand serves as a tridentate ligand, and the twisted ligands provide one pyridine N and one phenolate O atom, respectively. The bond distances of Co2-N/O are in the range of 2.018(3) – 2.137(3) Å, except Co2-N4 = 2.397(4) Å. The bond angles of cis N–Co2–O/N vary from 59.88(14) to 109.48(13)°, which deviates substantially from an ideal octahedral geometry. Co1 and Co2 are triply connected by two phenolate-O bridges with Co1-O1/O2-Co2 = 94.30(0)/93.02(0)°, respectively, and one syn-syn N–C–N bridge, leading to Co1–Co2 distance of 3.036(1) Å- slightly shorter than that (3.049(3) Å) in **2**. It should be mentioned that the smaller bridging angle (92.19(10)°) of Co1-O2-Co2 in **2** may be due to H-bonding between O2 and N6. Each molecule in **1** is well isolated with the nearest intermolecular neighbor giving a Co…Co distance of 8.541(3) Å, which is significantly longer than that of 7.351 Å in **2** (Fig. S4).

Magnetic properties

Variable-temperature direct-current (dc) magnetic susceptibility measured in an applied field of 1 kOe for both **1** and **2** is shown in Fig. 2. The χ_mT value of ca. 8.95 and 8.70 cm^3 mol^{-1} K for **1** and **2**, respectively, at 300 K, is much higher than the spin-only value (5.625 cm^3 mol^{-1} K) for three isolated HS Co^{II} metal ions, indicating significant spin-orbital couplings present.[19] For **1**, the χ_mT value increases steadily upon cooling to a maximum of 14.1 cm^3 mol^{-1} K at 6 K, suggesting significant ferromagnetic (*F*) couplings between the neighbouring Co(II) ions, then slightly decreases to 13.5 cm^3 mol^{-1} K at 2 K, likely due to the zero-field splitting effect and/or intermolecular antiferromagnetic (*AF*) interactions. For **2**, the χ_mT value decreases gradually to 7.7 cm^3 mol^{-1} K at ca. 20 K and then increases slightly to a maximum of 8.0 cm^3 mol^{-1} K at 9 K before dropping again. This curve suggests much weaker couplings within **2**. The data may be fit by using the PHI program[20] with the Hamiltonian as the following equation (eq. 1) as well as the mean-field approximation (eq. 2):

$$H = -2J(\hat{S}_1 \cdot \hat{S}_2 + \hat{S}_2 \cdot \hat{S}_3) + \sum_{i=1}^{3}\{D_i(\hat{S}_{i,z}^2 - \hat{S}_i(\hat{S}_i+1)/3) + E_i(\hat{S}_{i,x} - \hat{S}_{i,y}^2) + \mu_B g \hat{S}_i \hat{B}\} \quad \text{(eq. 1)}$$

$$\chi_{\exp} = \frac{\chi_{calc}}{1 - (\frac{2zJ}{N_A \mu_B^2 g^2})\chi_{calc}} \quad \text{(eq. 2)}$$

where μ_B, J, zJ, D_i, E_i, S_i, B, N_A correspond to the Bohr magneton, the intracluster and intercluster interaction, the axial and rhombic ZFS parameters, the spin operator, the magnetic field vector, and Avogadro's constant, respectively. The best simulations are found: for **1**, J = 2.4 cm^{-1}, g_{iso} = 2.48, D_{Co} = -27.0 cm^{-1}, E = 0, and zJ = -0.04 cm^{-1}; for **2**, J = 0.65 cm^{-1}, g_{iso} = 2.46, D_{Co} = -28.5 cm^{-1}, E = 0, and zJ = -0.14 cm^{-1}. On the basis of the J value, the first excited state (S = 7/2) may be well isolated with an approximate energy gap of 7.2 cm^{-1} (3J) from the ground state (S_T = 9/2) in **1**; while the states may be heavily mixed in **2** due to the weaker couplings. To date, structure-magneto correlation for the anisotropic Co(II) system is still not clear, because of the complications arising from orbital contributions, which are highly dependent on the coordination geometry, as well as ligand field around the metal center.[13b,21] One purported hypothesis that has gained general acceptance suggests that larger Co-O-Co angles would allow for antiferromagnetic (AF) exchange while smaller angles correspond to ferromagnetic (F) exchange.[21] As such, a crossover angle corresponding to AF/F transfer is likely to exist, which may explain our observed significant change on the J

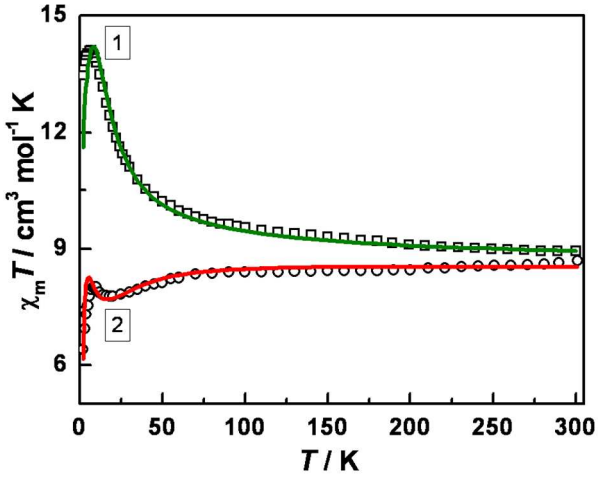

Fig. 2 χ_mT vs. T in an applied field of 1 kOe for **1** and **2:** the solid lines represent the best simulations via a linear trimeric model by PHI program.

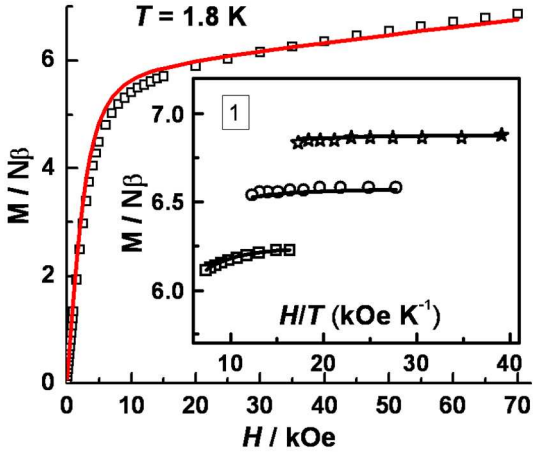

Fig. 3 M vs. H plot at 1.8 K for **1**. The solid line represents the simulation by PHI based on eq. 1 with J = 2.4 cm^{-1}, g_{iso} = 2.48, D_{Co} = -27.0 cm^{-1} and E = 0. Inset: Reduced magnetization data for **1** in applied fields (30, 50 and 70 kOe) at temperatures between 1.8 and 3.0 K; the solid lines represent the best fitting via ANISOFIT$^{2.0}$.

View Article Online
DOI: 10.1039/C4DT03545C

values, even though only a small variation exists in the related bridging angles [∠Co1-O1/O2-Co2 = 94.30(0)/93.02(0)° for **1** and 94.61(9)/92.19(9)° for **2**]. Furthermore, the different donor ligand strength (σ-donor (MeOH) in **1** and π-donor (pya) in **2**) may also play a vital role.[22] However, our attempts on replacing pya with methanol in **2** or methanol with pya in **1** did not succeed.

The isothermal magnetization (*M*) as a function of the applied field (*H*) was collected at 1.8 K for both **1** and **2** (Fig.s 3 and S5). The magnetization did not saturate up to 7.0 T and the values of 6.9 Nβ and 6.5 Nβ for **1** and **2**, respectively, are substantially smaller than the expected value (> 9.0 Nβ) when g > 2.0 for an S_T = 9/2 magnetic ground state. This behaviour indicated strong magnetic anisotropy, which was further confirmed by the reduced magnetizations measured in the range of 1.8 to 3.0 K at applied fields of 3, 5 and 7 T, where the isofield lines are non-superimposable (Inset of Fig.s 3 and S5). The best fit to the data by using Anisofit 2.0[23] for a S_T = 9/2 spin model gave: for **1**, D = −6.5 cm^{-1}, E = 0.009 cm^{-1}, and g_{iso} = 2.56 with R = 9.4 × 10^{-5}; for **2**, D = -2.3 cm^{-1}, E = 0.016 cm^{-1}, and g_{iso} = 2.05 with R = 1.1 × 10^{-3} {R = $\sum(M_{exp}-M_{fit})^2/\sum(M_{exp}^2)$}. The resulting smaller g_{iso} value for **2** demonstrated that the spin model (S_T = 9/2) may not be suitable due to the weaker intracluster interactions. It should be mentioned that the D value for **1** is among the largest for all cluster-based SMMs,[9a,24] and may lead to an energy barrier of U = 130 cm^{-1}. Additionally, the simulation by using the same set of parameters (*vide supra*) for M-T data roughly matches with the *M-H* data for **1**, however, the effort to extract reasonable parameters for **2** did not succeed. Interestingly, the extracted global molecular D (-6.5 cm^{-1}) and the single ion D_{Co} (-27.0 cm^{-1}) for **1** follows the calculated expression of $D(9/2) \approx 0.25D_{Co}$.[25] It may be mentioned that no hysteresis loop of magnetization was observed for **1** at 1.9 K (Fig. S6).

To probe the magnetization dynamics of **1** and **2**, ac susceptibility data was collected at different frequencies and under zero and nonzero static fields below 5 K. Frequency dependent ac susceptibility for **1** at zero dc field reveal the beginning of out-of-phase signals, although no maxima are observed (Fig. S7). As Co(II)-SMMs are known to show a high prevalence of fast quantum tunnelling at zero field, applied dc fields could efficiently reduce this probability.[8] Additional ac measurements were collected under small dc fields (H_{dc} ≤ 1500 Oe) at 1.8 K (Fig. S8). As expected, the relaxation in magnetization was dramatically decreased even under a very small dc field with the characteristic frequency (maximum in the χ_m'' vs ν plot) appearing at ~110 Hz (300 Oe), and 65 Hz (500 Oe), etc. The Cole–Cole plots fitted by the generalized Debye model[26] gave α parameters of 0.14-0.19 and relaxation times from 1.2 × 10^{-3} to 1.3 × 10^{-3} s (Fig. S9, Table S1).

Detailed ac magnetic susceptibility for **1** was measured as a function of both temperature (1.8 – 4.0 K) and frequency (1-1500 Hz) in an applied dc field of 500 Oe. Remarkably, strong frequency-dependent peaks in both in-phase and out-of-phase components of the susceptibility appear below 4 K with the peaks for 1400 Hz occurring at ~2.5 K and 100 Hz at ~1.9 K (Fig. 4a). The ratio (χ_m':χ_m'' ≈ 3:1) is in agreement with other well-established SMMs.[7] The shift of peak temperature (T_p) in χ_m'' is measured by the parameter $\phi = (\Delta T_p/T_p)/\Delta(\log f) \approx 0.20$, which also confirms super paramagnetic behaviour.[27] Variable-

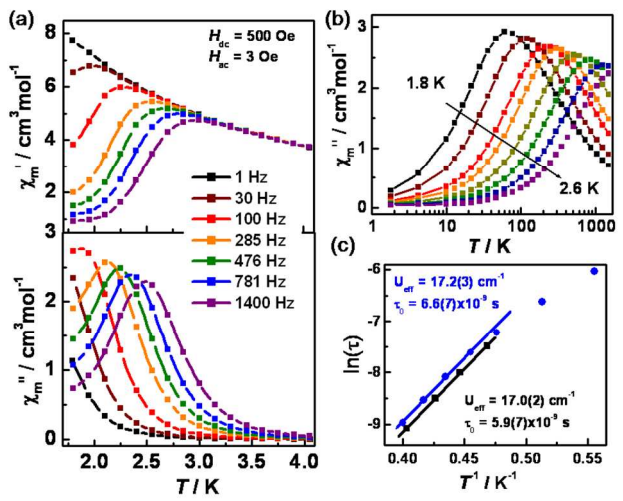

Fig. 4 (a) Variable-temperature and (b) variable-frequency in-phase and out-of-phase components of the ac magnetic susceptibility data for **1**, collected at temperatures of 1.8 – 2.6 K with a dc applied field of 500 Oe and ac field of 3 Oe; (c) Arrhenius plot of relaxation time, as determined through variable temperature (black) and variable-frequency (blue) ac susceptibilities.

frequency data collected in the temperatures 1.8 – 2.6 K show highly frequency dependent peaks (Fig. 4b). The relaxation time follows an Arrhenius law: $\tau = \tau_0 \exp(U_{eff}/k_BT)$ with an energy gap, U_{eff} = 17.2(3) cm^{-1} and τ_0 = 6.6(7) × 10^{-9} s (Fig. 4c). The energy barrier and pre-exponential constant are comparable with those of previously reported Co(II)-SMMs as well as [$Co^{II}_2Gd^{III}$] SMM under an applied dc field.[14b] The significant increase for the characteristic frequency-dependence under dc fields confirms the presence of strong quantum tunnelling at zero field. However, the effective barrier height is still far lower than the calculated value (-130 cm^{-1}, *vide supra*), indicating that the quantum tunnelling effect is the predominant relaxation mode. The Cole–Cole plots (Fig. S10) of **1** at temperatures between 1.80 and 2.60 K exhibit a symmetric shape and can be fit to the generalized Debye model, with α parameters of 0.08-0.18 (Table S2), which supports a relative narrow distribution of relaxation times.[26]

For compound **2**, in the absence of an applied dc field, no out-of-phase (χ'') signals were observed at frequencies up to 9999 Hz and temperatures down to 1.8 K. However, under a 1 kOe applied field, strong frequency-dependent tails of χ'' appear, suggesting SMM behaviour with fast quantum tunnelling (Fig. S11).

For comparison, rough estimations of U_{eff} and τ_0 for both **1** and **2** by fitting the experimental data at 4111 Hz based on a relative expression suitable for cluster compounds with only one characteristic relaxation process:[28] $\ln(\chi''/\chi') = \ln(\omega\tau_0)+U_{eff}/(k_BT)$, gave U_{eff} (1 kOe) = 18.0(2) cm^{-1} and τ_0 = 1.9 × 10^{-8} s for **1** and U_{eff} (1kOe) = 7.9(1) cm^{-1} and τ_0 = 8.5 × 10^{-8} s for **2** (Fig. S12). We presumptively attribute the slow relaxation in **2** to single-ion behavior instead of cluster behavior due to the weak couplings. As a result, the effective energy barrier for **1** is two times higher than that for **2**. Overall, this work gives evidence for the potential co-alignment of the anisotropy tensors in linear trinuclear systems - making them an ideal target for large global anisotropy.[29]

Conclusions

View Article Online
DOI: 10.1039/C4DT03545C

In summary, we characterized the first linear trinuclear $[Co^{II}_3]$ SMM with an effective energy barrier of 17.2(3) cm^{-1} under 500 Oe dc field and found significant ferromagnetic couplings (J = +2.4 cm^{-1}) in **1**. Our result suggests that even a slight change in the coordination environments of the cobalt centers have a distinct influence on the magnetic properties.

Acknowledgments

This work was supported by NSFC (21321001) and the National Basic Research Program of China (2013CB933400).

Notes and references

[a] *Beijing National Laboratory for Molecular Sciences, State Key Laboratory of Rare Earth Materials Chemistry and Applications, College of Chemistry and Molecular Engineering, Peking University, 100871 Beijing, China. E-mail: gaosong@pku.edu.cn; yuanzhuzhang@gmail.com.*
[b] *Department of Chemistry, Texas A & M University, College Station, TX 77842-3012 (USA).*
[c] *Department of Chemistry, Beijing Normal University, Beijing 100875, P. R. China*

† Electronic Supplementary Information (ESI) available: additional magnetic data of **1** and **2**. CCDC-823183 for **1** contains the supplementary crystallographic data can be also obtained free of charge at www.ccdc.cam.ac.uk/data_request/cif.

1 D. Gatteschi and R. Sessoli, *Angew. Chem. Int. Ed.* 2003, **42**, 268.
2 (a) O. Waldmann, *Inorg. Chem.* 2007, **46**, 10035; (b) F. Neese and D. A. Pantazis, *Dalton Trans.* 2011, **148**, 229.
3 C. J. Milios, A. Vinslava, W. Wernsdorfer, S. Moggach, S. Parsons, S. P. Perlepes, G. Christou and E. K. Brechin, *J. Am. Chem. Soc.* 2007, **129**, 2754.
4 J. Vallejo, A. Pascual-Alvarez, J. Cano, I. Castro, M. Julve, F. Lloret, J. Krzystek, G. De Munno, D. Armentano, W. Wernsdorfer, R. Ruiz-Garcia and E. Pardo, *Angew. Chem. Int. Ed.* 2013, **52**, 14075.
5 D. N. Woodruff, R. E. P. Winpenny and R. A. Layfield, *Chem. Rev.* 2013, **113**, 5110.
6 (a) J. M. Zadrozny, D. J. Xiao, M. Atanasov, G. J. Long, F. Grandjean, F. Neese and J. R. Long, *Nat. Chem.* 2013, **5**, 577; (b) P. H. Lin, N. C. Smythe, S. I. Gorelsky, S. Maguire, N. J. Henson, I. Korobkov, B. L. Scott, J. C. Gordon, R. T. Baker and M. Murugesu, *J. Am. Chem. Soc.* 2011, **133**, 15806; (c) D. E. Freedman, W. H. Harman, T. D. Harris, G. J. Long, C. J. Chang and J. R. Long, *J. Am. Chem. Soc.* 2010, **132**, 1224; (d) S. Mossin, B. L. Tran, D. Adhikari, M. Pink, F. W. Heinemann, J. Sutter, R. K. Szilagyi, K. Meyer and D. J. Mindiola, *J. Am. Chem. Soc.* 2012, **134**, 13651; (e) R. Ruamps, R. Maurice, L. Batchelor, M. Boggio-Pasqua, R. Guillot, A. L. Barra, J. J. Liu, E. Bendeif, S. Pillet, S. Hill, T. Mallah and N. Guihery, *J. Am. Chem. Soc.* 2013, **135**, 3017; (f) R. C. Poulten, M. J. Page, A. G. Algarra, J. J. Le Roy, I. López, E. Carter, A. Llobet, S. A. Macgregor, M. F. Mahon, D. M. Murphy, M. Murugesu and M. K. Whittlesey, *J. Am. Chem. Soc.* 2013, **135**, 13640.
7 M. Murrie, *Chem. Soc. Rev.* 2010, **39**, 1986 and references therein.
8 (a) M. R. Saber and K. R. Dunbar, *Chem. Commun.* 2014; (b) R. Ruamps, L. J. Batchelor, R. Guillot, G. Zakhia, A.-L. Barra, W. Wernsdorfer, N. Guihery and T. Mallah, *Chem. Sci.* 2014, **5**, 3418; (c) R. Herchel, L. Váhovská, I. Potočňák and Z. Trávníček, *Inorg. Chem.* 2014, **53**, 5896; (d) R. Boča, J. Miklovič and J. Titiš, *Inorg. Chem.* 2014, **53**, 2367; (e) Y. Y. Zhu, C. Cui, Y. Q. Zhang, J. H. Jia, X. Guo, C. Gao, K. Qian, S. D. Jiang, B. W. Wang, Z. M. Wang and S. Gao, *Chem. Sci.* 2013, **4**, 1802; (f) J. M. Zadrozny, J. Telser and J. R. Long, *Polyhedron*, 2013, **64**, 209; (g) F. Yang, Q. Zhou, Y. Zhang, G. Zeng, G. Li, Z. Shi, B. Wang and S. Feng, *Chem. Commun.* 2013, **49**, 5289; (h) R. Ruamps, L. J. Batchelor, R. Maurice, N. Gogoi, P. Jimenez-Lozano, N. Guihery, C. de Graaf, A. L. Barra, J. P. Sutter and T. Mallah, *Chem-Eur J*, 2013, **19**, 950; (i) M. Idešicová, J. Titiš, J. Krzystek and R. Boča, *Inorg. Chem.* 2013, **52**, 9409; (j) W. Huang, T. Liu, D. Wu, J. Cheng, Z. W. Ouyang and C. Duan, *Dalton Trans*, 2013, **42**, 15326; (k) F. Habib, O. R. Luca, V. Vieru, M. Shiddiq, I. Korobkov, S. I. Gorelsky, M. K. Takase, L. F. Chibotaru, S. Hill, R. H. Crabtree and M. Murugesu, *Angew. Chem. Int. Ed.* 2013, **52**, 11290; (l) J. M. Zadrozny, J. J. Liu, N. A. Piro, C. J. Chang, S. Hill and J. R. Long, *Chem. Commun.* 2012, **48**, 3927; (m) J. Vallejo, I. Castro, R. Ruiz-García, J. Cano, M. Julve, F. Lloret, G. De Munno, W. Wernsdorfer and E. Pardo, *J. Am. Chem. Soc.* 2012, **134**, 15704; (n) S. A. Cantalupo, S. R. Fiedler, M. P. Shores, A. L. Rheingold and L. H. Doerrer, *Angew. Chem. Int. Ed.* 2012, **51**, 1000; (o) J. M. Zadrozny and J. R. Long, *J. Am. Chem. Soc.* 2011, **133**, 20732; (p) D. Weismann, Y. Sun, Y. Lan, G. Wolmershäuser, A. K. Powell and H. Sitzmann, *Chem. – Eur. J.*, 2011, **17**, 4700; (q) T. Jurca, A. Farghal, P. H. Lin, I. Korobkov, M. Murugesu and D. S. Richeson, *J. Am. Chem. Soc.* 2011, **133**, 15814.
9 (a) I.-R. Jeon, J. G. Park, D. J. Xiao and T. D. Harris, *J Am Chem Soc*, 2013, **135**, 16845; (b) S. Fortier, J. J. Le Roy, C.-H. Chen, V. Vieru, M. Murugesu, L. F. Chibotaru, D. J. Mindiola and K. G. Caulton, *J. Am. Chem. Soc.* 2013, **135**, 14670; (c) S. Demir, J. M. Zadrozny, M. Nippe and J. R. Long, *J. Am. Chem. Soc.* 2012, **134**, 18546.
10 (a) E.-C. Yang, D. N. Hendrickson, W. Wernsdorfer, M. Nakano, L. N. Zakharov, R. D. Sommer, A. L. Rheingold, M. Ledezma-Gairaud and G. Christou, *J. Appl. Phys.* 2002, **91**, 7382; (b) K. W. Galloway, A. M. Whyte, W. Wernsdorfer, J. Sanchez-Benitez, K. V. Kamenev, A. Parkin, R. D. Peacock and M. Murrie, *Inorg. Chem.* 2008, **47**, 7438.
11 Q. Chen, M.-H. Zeng, Y.-L. Zhou, H.-H. Zou and M. Kurmoo, *Chem. Mater.* 2010, **22**, 2114.
12 (a) Y. Z. Zhang, W. Wernsdorfer, F. Pan, Z. M. Wang and S. Gao, *Chem. Commun.* 2006, 3302; (b) X.-T. Wang, B.-W. Wang, Z.-M. Wang, W. Zhang and S. Gao, *Inorg. Chim. Acta,* 2008, **361**, 3895.
13 (a) A. Ferguson, A. Parkin, J. Sanchez-Benitez, K. Kamenev, W. Wernsdorfer and M. Murrie, *Chem. Commun.* 2007, 3473; (b) M. Moragues-Canovás, C. E. Talbot-Eeckelaers, L. Catala, F. Lloret, W. Wernsdorfer, E. K. Brechin and T. Mallah, *Inorg. Chem.* 2006, **45**, 7038.
14 (a) V. Chandrasekhar, B. M. Pandian, J. J. Vittal and R. Clérac, *Inorg. Chem.* 2009, **48**, 1148; (b) V. Chandrasekhar, B. M. Pandian, R. Azhakar, J. J. Vittal and R. Clérac, *Inorg. Chem.* 2007, **46**, 5140.
15 Y.-Z. Zheng, M. Speldrich, H. Schilder, X.-M. Chen and P. Kogerler, *Dalton Trans*, 2010, **39**, 10827.
16 X. Lin, J. Tao, R.-B. Huang and L.-S. Zheng, *Inorg. Chem. Commun.* 2009, **12**, 154.
17 H. L. Zhu and X. Y. Liu, *Syn. React. Inorg. Met.-Org, Nano-Met. Chem.* 2005, **35**, 193.
18 G. A. Bain and J. F. Berry, *J. Chem. Edu.*, 2008, **85**, 532.
19 O. Kahn, *Molecular Magnetism,* VCH: New York, NY, 1993.
20 N. F. Chilton, R. P. Anderson, L. D. Turner, A. Soncini and K. S. Murray, *J. Comput. Chem.* 2013, **34**, 1164.
21 (a) G. A. Seisenbaeva, M. Kritikos and V. G. Kessler, *Polyhedron*, 2003, **22**, 2581; (b) G. A. Seisenbaeva, T. Mallah and V. G. Kessler, *Dalton Trans.* 2010, **39**, 7774; (c) D. Aguila, L. A. Barrios, O. Roubeau, S. J. Teat and G. Aromi, *Chem. Commun.* 2011, **47**, 707.
22 H. I. Karunadasa, K. D. Arquero, L. A. Berben and J. R. Long, *Inorg. Chem.* 2010, **49**, 4738.
23 M. P. Shores, J. J. Sokol and J. R. Long, *J. Am. Chem. Soc.* 2002, **124**, 2279.
24 C. F. Wang, J. L. Zuo, B. M. Bartlett, Y. Song, J. R. Long and X. Z. You, *J. Am. Chem. Soc.* 2006, **128**, 7162.
25 O. Waldmann, *Inorg. Chem.*, 2007, **46**, 10035.
26 R. Schenker, M. N. Leuenberger, G. Chaboussant, D. Loss and H. U. Gudel, *Phys. Rev. B*, 2005, **72**.
27 S. M. J. Aubin, Z. Sun, L. Pardi, J. Krzystek, K. Folting, L.-C. Brunel, A. L. Rheingold, G. Christou and D. N. Hendrickson, *Inorg. Chem.* 1999, **38**, 5329.
28 J. Bartolome, G. Filoti, V. Kuncser, G. Schinteie, V. Mereacre, C. E. Anson, A. K. Powell, D. Prodius and C. Turta, *Phys. Rev. B.* 2009, **80**, 014430.
29 Y. Z. Zhang, U. P. Mallik, N. P. Rath, R. Clerac and S. M. Holmes, *Inorg. Chem.* 2011, **50**, 10537.

View Article Online
DOI: 10.1039/C4DT03545C

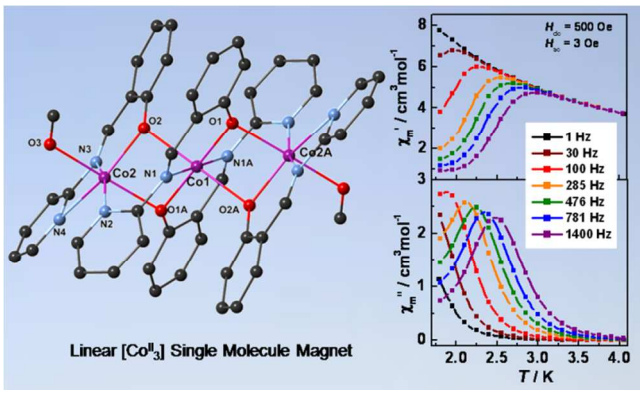

The first linear trinuclear [Co$^{II}_3$] SMM is achieved due to significant intracluster ferromagnetic couplings. This study highlights that miniscule changes in the coordination environment of the cobalt centers in this structural archetype can have a drastic effect on the observation of SMM behavior.